

# A Constant-Gain Equation-Error Framework for Airliner Aerodynamic Monitoring Using QAR Data

Ruiying Wen<sup>a</sup>, Yuntao Dai<sup>\*,a</sup>, Hongyong Wang<sup>a</sup>

<sup>a</sup>*Civil Aviation University of China, Jinbei Highway 2898, Dongli District, Tianjin, 300300, Tianjin, China*

---

## Abstract

Monitoring the in-service aerodynamic performance of airliners is critical for operational efficiency and safety, but using operational Quick Access Recorder (QAR) data for this purpose presents significant challenges. This paper first establishes that the absence of key parameters, particularly aircraft moments of inertia, makes conventional state-propagation filters fundamentally unsuitable for this application. This limitation necessitates a decoupled, Equation-Error Method (EEM). However, we then demonstrate through a comparative analysis that standard recursive estimators with time-varying gains, such as Recursive Least Squares (RLS), also fail within an EEM framework, exhibiting premature convergence or instability when applied to low-excitation cruise data. To overcome these dual challenges, we propose and validate the Constant-Gain Equation-Error Method (CG-EEM). This framework employs a custom estimator with a constant, Kalman-like gain, which is perfectly suited to the stationary, low-signal-to-noise characteristics of cruise flight. The CG-EEM is extensively validated on a large, multi-fleet dataset of over 200 flights, where it produces highly consistent, physically plausible aerodynamic parameters and correctly identifies known performance differences between aircraft types. The result is a robust, scalable, and computationally efficient tool for fleet-wide performance monitoring and the early detection of performance degradation.

**Keywords:** Parameter estimation, System identification, Quick Access Recorder (QAR), Constant-Gain Kalman Filter (CGKF), Recursive Least Square (RLS)

---

## 1. Introduction

An aircraft's aerodynamic characteristics are not static; they evolve throughout its operational life. Factors such as structural aging, engine wear, and surface roughness from paint degradation or contamination can significantly alter performance from the original design specifications. Furthermore, modifications like the installation of new antennas can introduce unexpected aerodynamic penalties. Research has quantified these effects, showing that coating degradation can increase cruise drag by up to 7.1% on a Boeing 737-NG, while a fuselage-mounted Wi-Fi antenna can add another 1.92% [1]. This "performance drift" directly impacts fuel efficiency and can alter handling qualities, underscoring the critical need for methods capable of continuously monitoring an aircraft's true aerodynamic state. Fortunately, modern airliners record a wealth of data using systems like the Quick Access Recorder (QAR), presenting a vast, yet largely untapped, resource for addressing this challenge.

Traditionally, Aerodynamic Parameter Estimation (APE) has relied on dedicated flight testing and computational fluid dynamics (CFD) [2, 3, 4, 5]. While these "gold-standard" approaches

provide high-fidelity results, they are too resource-intensive for routine monitoring, creating a need for methods that can leverage in-service operational data.

Two modern paradigms have emerged to fill this gap. The first, purely data-driven modeling using neural networks, has shown promise in capturing complex aerodynamic relationships [6, 7, 8, 9]. However, their "black-box" nature presents a major obstacle to certification and physical interpretation in safety-critical aviation [10]. The second paradigm, a physics-informed filtering approach, has centered on joint-estimation filters, mainly Kalman filters and their mutations [11, 12, 13, 14]. These methods attempt to simultaneously estimate both the aircraft state and its aerodynamic parameters. However, they rely on propagating the aircraft state through a dynamic model, which faces a fundamental barrier in a real-world operational context. Accurate state propagation, particularly of rotational dynamics, requires the aircraft's moments and products of inertia. These mass properties change continuously with fuel burn and are not recorded in standard QAR data, making a rigorous physics-based state propagation model impossible to implement. This unresolvable model error renders such coupled-filtering approaches fundamentally unsuitable for this specific application.

The limitations of state-propagation filters thus necessitate a decoupled, Equation-Error Method (EEM). In an EEM framework, the estimation problem is simplified by using the measured states from QAR data directly as inputs to an algebraic model of the aerodynamic forces, bypassing the need for dynamic propagation. The most common algorithm for such problems is the standard Recursive Least Squares (RLS) estimator.

However, a critical analysis reveals that conventional RLS is also not suited for this application due to the nature of its time-varying gain. RLS is designed to progressively reduce its estimation gain as it processes more data, effectively giving more weight to initial samples. In the context of noisy and low-excitation cruise data, this behavior is detrimental. The estimator can prematurely converge on inaccurate parameters based on initial sensor noise, or become less sensitive before it has processed enough data to find the true underlying signal. While a forgetting factor can be used to keep the gain from vanishing, this often leads to instability, causing the parameter estimates to drift and chase noise rather than converge.

To overcome these dual challenges, this paper proposes and validates the Constant-Gain Equation-Error Method (CG-EEM). Our framework is built on the robust EEM principle to bypass the need for unavailable aircraft parameters. Crucially, it replaces the standard time-varying gain estimator with a custom-designed, constant-gain algorithm inspired by the Constant-Gain Kalman Filter (CGKF) [14]. This approach is perfectly suited to extracting precise parameter estimates from long segments of stationary, noisy data by ensuring every data point contributes consistently to the final result. The primary contributions of this work are:

1. The development of CG-EEM, a robust framework for aerodynamic estimation designed specifically for the constraints and characteristics of operational QAR data.
2. A rigorous, simulation-based comparative analysis demonstrating that the CG-EEM is superior to conventional time-varying gain RLS for this application, avoiding both premature convergence and noise-induced instability.
3. Extensive validation of the framework on a large, multi-fleet dataset of over 200 flights, confirming its consistency, scalability, and ability to produce physically meaningful aerodynamic parameters for fleet-wide performance monitoring.

## 2. Quick Access Recorder (QAR) Data

Modern commercial airliners generate vast quantities of operational data through systems designed for proactive monitoring, complementing the traditional post-accident recorders (FDR and CVR). The primary source for this data is the Quick Access Recorder (QAR), which records thousands of flight parameters at high fidelity. The evolution of this technology to the Wireless QAR (WQAR) has automated post-flight data retrieval, while future systems may provide in-flight data transmission, further enhancing monitoring capabilities. For analysis, this data is decoded from its proprietary binary format and commonly stored in HDF5 files. This format is ideal as it preserves not only the time-series measurements but also essential metadata, including sensor units and data types. The key parameters leveraged in this study are summarized in Table 1.

Despite its richness, using raw QAR data for accurate Aerodynamic Parameter Estimation (APE) presents several fundamental challenges that preclude the direct application of standard system identification techniques:

1. **Sensor Noise and Quantization:** Onboard sensors, while adequate for flight operations, have inherent precision and granularity limitations. Figure 1 provides a stark illustration of this problem, comparing the aircraft's measured pitch angle with the time-integral of the raw pitch rate signal. The significant drift and divergence of the integrated signal demonstrate how even small amounts of sensor noise are amplified through integration, leading to physically inconsistent results. Any robust APE framework must effectively avoid the detrimental effects of this measurement noise.
2. **Lack of Critical Model Parameters:** Established APE frameworks, particularly those based on full non-linear equations of motion, often require parameters that are not explicitly recorded in QAR data. The most significant of these include manufacturer-specific thrust data and, crucially, the aircraft's moments and products of inertia. Without these, accurate state propagation for dynamic models is fundamentally infeasible, rendering coupled-estimation approaches (as discussed in Section 1) unsuitable.
3. **Low Persistent Excitation:** Operational flight data, particularly during quasi-steady, level cruise segments, lacks the dynamic variation typically needed for many estimators to converge. Dedicated flight tests are designed with specific maneuvers (e.g., doublets, frequency sweeps) to deliberately excite dynamic modes. In contrast, the vast majority of operational data is recorded during trim conditions, providing limited information content per sample. Any framework intended for routine monitoring must therefore be robust enough to extract meaningful information from these less-than-ideal conditions.

## 3. The Constant-Gain Equation-Error Method (CG-EEM) Framework

This section details the framework developed to identify aerodynamic parameters from in-service QAR data. The methodology is named the Constant-Gain Equation-Error Method (CG-EEM) to reflect its two core design principles, which were chosen specifically to overcome the data limitations discussed in Section 2. The overall architecture of the framework is depicted in Figure 2 and consists of three main stages: Data Extraction, Parameter Estimation, and Convergence Analysis.

Table 1: Explanation and nomenclature of QAR data used in this paper.

QAR Code	Physical Meaning	Unit	Symbol	Granularity	Sampling frequency
TAS	True Air Speed	knots	$V$	0.0001	Computed
GW	Gross Weight	lbs	$m$	0.0001	1/64 Hz
VRTG	Vertical g-acceleration	g	$a_z$	0.0039	16 Hz
LONG	Longitudinal g-acceleration	g	$a_x$	0.0039	16 Hz
PITCH	Pitch Angle	$^\circ$	$\theta$	0.0001	4 Hz
FLT_PATH	Flight Path Angle	$^\circ$	$\gamma$	0.0001	1 Hz
PITCH_RATE	Pitch Rate	$^\circ/\text{s}$	$q$	0.0001	8 Hz
TAT	Total Air Temperature	$^\circ\text{C}$	$T$	0.25	1 Hz
DRIFT	Drift Angle	$^\circ$	$\beta_d$	0.0039	4 Hz
WIN_SPD	Wind Speed	knots	$V_w$	1.0	2 Hz
WIN_DIR	Wind Direction	$^\circ$	$\delta$	0.0039	2 Hz
N11	Low Spool Speed of the Engine#1	%	$N11$	0.125	1/4 Hz
N12	Low Spool Speed of the Engine#2	%	$N12$	0.125	1/4 Hz
FF1	Fuel Flow of the Engine#1	lbs/h	$f_1$	0.001	1 Hz
FF2	Fuel Flow of the Engine#2	lbs/h	$f_2$	0.001	1 Hz
AOAL	Angle of Attack Left	$^\circ$	$\alpha_l$	0.3516	4 Hz
AOAR	Angle of Attack Right	$^\circ$	$\alpha_r$	0.3516	4 Hz

\*Note: computed data usually demonstrated in 1 Hz.

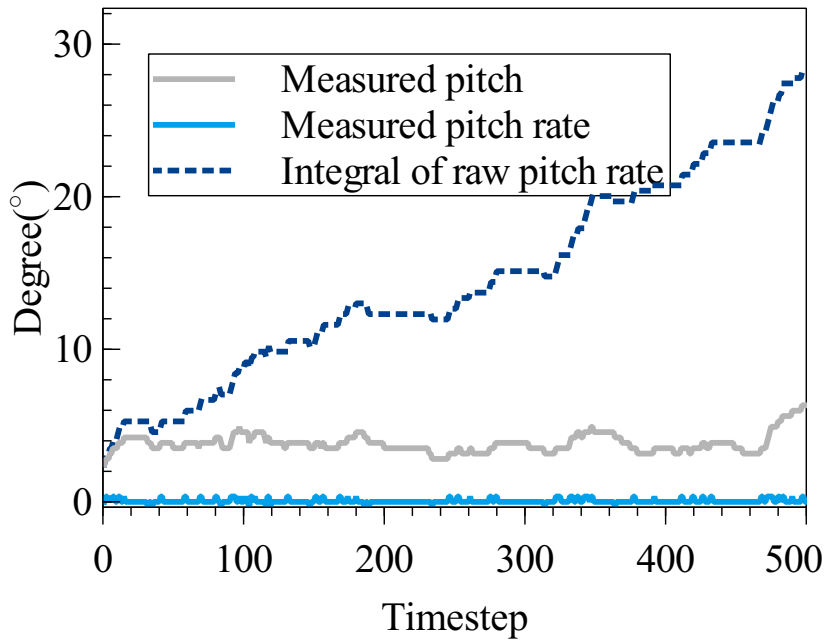


Figure 1: Comparison of integrated pitch rate and measured pitch angle, demonstrating significant deviation due to sensor noise.

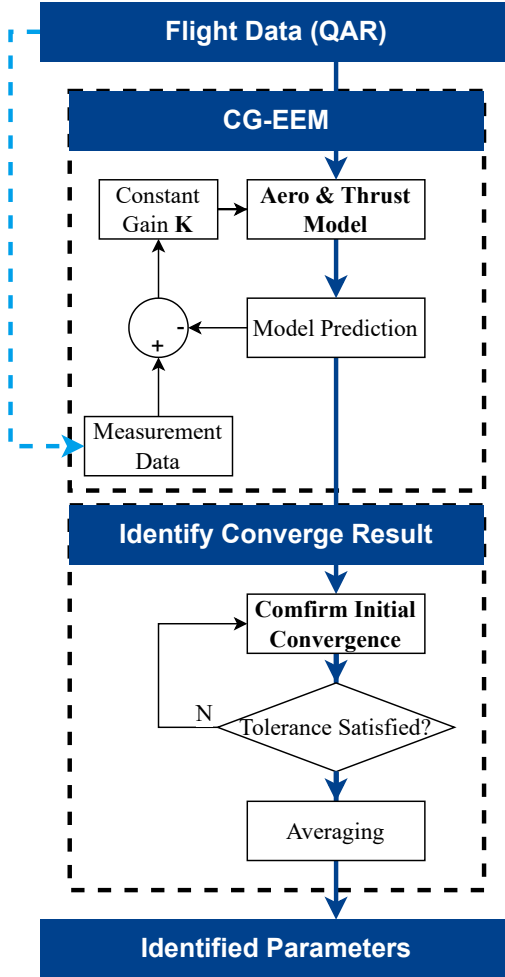


Figure 2: Flowchart of the proposed aerodynamic parameter identification framework, from raw QAR data to final identified aerodynamic parameters.

### 3.1. The Decoupled Equation-Error Formulation

The CG-EEM framework is built upon a decoupled, equation-error formulation. As established in Section 2, the absence of key parameters like moments of inertia in QAR data makes state propagation models infeasible. The equation-error approach bypasses this fundamental problem entirely. Instead of propagating states, the framework uses the measured states from the QAR data ( $\alpha, q, \theta, V$ ) directly as inputs to an algebraic model of the aircraft's forces. The esti-

mation task is thus simplified to identifying the parameters of this force model that best explain the measured longitudinal acceleration  $a_x$  and vertical acceleration  $a_z$ .

### 3.1.1. State and Parameter Vectors

The longitudinal motion of the aircraft is described by a state vector  $\mathbf{x}$ :

$$\mathbf{x} = [\alpha, q, \theta, V]^T \quad (1)$$

where  $\alpha$  is the angle of attack,  $q$  is the pitch rate,  $\theta$  is the pitch angle, and  $V$  is the true airspeed.

The aerodynamic model is defined by a vector of parameters  $\Theta$  to be estimated. Based on a standard polynomial representation of the aircraft's forces and moments, the parameter vector is defined as:

$$\Theta = [C_{L0}, C_{La}, C_{LM}, C_{D0}, C_{DL}, C_{TV}]^T \quad (2)$$

This vector includes coefficients for lift, drag, and a term for calculating the thrust of the engine.

### 3.1.2. Aerodynamic and Thrust Model

Aerodynamic forces (lift  $L$ , drag  $D$ ) are calculated at each time step. The model employs a linear structure for lift and a parabolic structure for drag, which is a standard and effective representation for conventional aircraft in the cruise phase of flight.

The Lift Coefficient  $C_L$  is modeled as:

$$C_L = C_{L0} + C_{La}\alpha + C_{LM}V_M \quad (3)$$

The Drag Coefficient  $C_D$  is modeled using the standard parabolic drag polar. This structure is chosen for its strong physical basis, representing drag as the sum of a baseline parasitic component  $C_{D0}$  and a lift-induced component that varies with the square of the lift coefficient  $C_L$ :

$$C_D = C_{D0} + C_{DL}C_L^2 \quad (4)$$

It is important to note that alternative drag model formulations were also investigated during this research, including those with linear dependencies on the angle of attack [11]. However, our analysis consistently showed that these alternative structures were unable to provide stable convergence and resulted in physically inconsistent force estimations, particularly in the longitudinal channel. The parabolic polar, which correctly links drag to the generation of lift, proved to be essential for achieving a globally consistent solution across both the longitudinal and vertical axes. Therefore, this physically-grounded model was selected for our final framework.

Since direct thrust measurements are unavailable in QAR data, engine thrust  $T$  is calculated from the measured fuel flow  $f$  and the mach speed  $V_M$ . The core of the model is the Thrust Specific Fuel Consumption (TSFC), which relates fuel consumption to the thrust produced. While TSFC is a complex function of altitude, Mach number, and engine settings, research has shown that for the specific case of high-altitude, quasi-steady cruise, its dependency simplifies significantly. As concluded by [15], we adopt a linear model for TSFC as a function of Mach speed, and therefore the thrust is calculated as:

$$T = \frac{f}{TSFC} \quad (5)$$

where  $TSFC$  is calculated by

$$TSFC = T_0 + C_{TV}V_M \quad (6)$$

In this formulation, the measured fuel flow  $f$  and Mach speed  $V_M$  are inputs from the QAR data. The unknown thrust coefficient  $C_{TV}$  is unknown and estimated simultaneously with the aerodynamic coefficients.

### 3.1.3. Measurement Model

The measurement vector  $\mathbf{z}$  consists of the available sensor readings. The measurement model,  $h(\mathbf{x}, \Theta)$ , predicts these sensor readings based on the current state and parameters.

$$\mathbf{z}_k = h(\mathbf{x}_k, \Theta_k) + \mathbf{v}_k \quad (7)$$

where  $\mathbf{v}_k$  is the measurement noise, assumed to be zero-mean Gaussian with covariance  $\mathbf{R}$ . The predicted measurement vector is:

$$\hat{\mathbf{z}}_k = [\alpha, q, \theta, V, a_x, a_z]^T \quad (8)$$

The longitudinal ( $a_x$ ) and vertical ( $a_z$ ) accelerations are calculated as:

$$a_x = \frac{-D \cos(\alpha) - L \sin(\alpha) + T \cos(\sigma)}{m} \quad (9)$$

$$a_z = \frac{-D \sin(\alpha) + L \cos(\alpha) + T \sin(\sigma)}{m} \quad (10)$$

where  $m$  is the aircraft mass and  $\sigma$  is the thrust line offset angle.

### 3.2. The Constant-Gain Parameter Estimator

The second core principle of the CG-EEM is the use of a constant-gain estimator. Standard Recursive Least Squares (RLS) was found to be unsuitable for this application because its time-varying gain diminishes too rapidly, leading to premature convergence on the low-excitation cruise data.

To address this, our estimator is designed to maintain a consistent, non-vanishing gain throughout the analysis window. While structured similarly to RLS, it differs in a crucial way: the parameter covariance matrix  $\mathbf{P}$  is not recursively updated. Instead, the apriori covariance  $\mathbf{P}'$  used for the gain calculation is reset at each time step  $k$  based on the initial uncertainty matrix  $\mathbf{P}_0$ . The update equations are as follows:

#### 1. Compute Measurement Residual (Error)

The error  $\mathbf{e}_k$  is the difference between the actual measurement  $\mathbf{z}_k$  and the measurement predicted using the parameters from the previous step,  $\Theta_{k-1}$ .

$$\mathbf{e}_k = \mathbf{z}_k - h(\mathbf{x}_k, \Theta_{k-1})$$

*Note: For this algorithm, the state vector  $\mathbf{x}_k$  is taken directly from the measured data at time  $k$ , not from a state propagation model.*

## 2. Compute Measurement Sensitivity Matrix (Jacobian)

The matrix  $\mathbf{H}_k$  describes how sensitive the predicted measurement is to a small change in each parameter. It is the partial derivative of the measurement function with respect to the parameter vector.

$$\mathbf{H}_k = \left. \frac{\partial h}{\partial \theta} \right|_{\mathbf{x}_k, \theta_{k-1}}$$

Due to the complexity of the model, this Jacobian is computed numerically at each step using finite differences.

## 3. Compute Gain with Constant Covariance

The parameter covariance matrix is invariant during whole process. And a Kalman-like gain,  $\mathbf{K}_k$ , is computed to blend the new information from the measurement residual with the current parameter estimate.

$$\mathbf{P}' = \mathbf{P}_0$$

$$\mathbf{S}_k = \mathbf{H}_k \mathbf{P}' \mathbf{H}_k^\top + \mathbf{R}$$

$$\mathbf{K}_k = \mathbf{P}' \mathbf{H}_k^\top \mathbf{S}_k^{-1}$$

## 4. Update Parameters

The parameters are then updated:

$$\boldsymbol{\Theta}_k = \boldsymbol{\Theta}_{k-1} + \mathbf{K}_k \mathbf{e}_k$$

### 3.3. Implementation and Tuning

The CG-EEM framework was implemented in the Julia programming language. The estimator requires tuning of two key matrices: the initial parameter covariance  $\mathbf{P}_0$  and the measurement noise covariance  $\mathbf{R}$ . The initial parameter covariance,  $\mathbf{P}_0$ , represents the uncertainty in the initial guess for the parameter vector  $\boldsymbol{\Theta}$ . It was initialized as a diagonal matrix with large values (e.g.,  $10^2$ ) on the diagonal. This signifies high initial uncertainty, allowing the estimator to freely adapt to the information in the data without being biased by its starting point.

The measurement noise covariance  $\mathbf{R}$  is a diagonal matrix representing the expected variance of the measurement noise. A sensitivity analysis was conducted to determine the effect of  $\mathbf{R}$  on the estimator's performance. It was found that the CG-EEM framework is remarkably robust to the choice of this parameter. For a typical initial parameter covariance  $\mathbf{P}_0$  with diagonal elements on the order of  $10^2$ , the final parameter estimates remained virtually unchanged for values of  $\mathbf{R}$  ranging from  $1e-3$  to  $1e1$ .

### 3.4. Convergence Criteria and Final Parameter Extraction

The CG-EEM estimator produces a time-series of parameter estimates for each analyzed flight segment. To enable robust statistical analysis across a fleet, a systematic and objective procedure was established to extract a single, representative value for each parameter. This process explicitly addresses the question of how to ensure the estimator has truly converged.

The procedure involves two steps. First, an initial transient period, corresponding to the first 60% of the time steps in a segment, is discarded. This allows the estimator ample time to move from its initial uninformed state towards a stable solution.

Second, convergence is objectively verified on the latter 40% of the segment, defined as the "convergence window". Certainty of convergence is not assumed; it is statistically tested. For each estimated parameter, the Coefficient of Variation (CV) is calculated within this window.

The CV, defined as the ratio of the standard deviation  $\sigma$  to the absolute mean  $|\mu|$ , is a normalized measure of dispersion:

$$CV = \frac{\sigma}{|\mu|} \quad (11)$$

An estimated parameter is considered to have successfully converged if its CV within the convergence window is less than a predefined threshold. The choice of this threshold accounts for the inherent identifiability of different physical effects. Based on the sensitivity and variance analysis presented in Section 4.1.2, a stricter threshold of 1% is used for the more readily identifiable lift-related parameters, while a threshold of 10% is used for the drag-related parameters, whose estimation is more sensitive to measurement noise.

This objective criterion ensures that the final value is not derived from a drifting or excessively noisy estimate. Flights containing segments where any parameter fails to meet its respective CV threshold are flagged for manual inspection. Such instances are typically associated with unmodeled dynamics, such as significant turbulence or banking maneuvers, which fall outside the scope of the quasi-steady flight assumption.

Once convergence is confirmed, the single representative value for each aerodynamic parameter is calculated as the mean of the estimates within this stable convergence window. This mean value is then used for all subsequent fleet-wide statistical analyses.

## 4. Results and discussion

This section presents the validation and application of the CG-EEM framework. First, integrity and superiority of the algorithm over alternatives are verified using a simulated dataset with a simulated known ground truth. The validated framework is then applied to a large dataset of operational QAR flights to demonstrate its performance and utility.

### 4.1. Verification on Simulated Data

Before its application to operational data, the CG-EEM framework was subjected to a rigorous verification study using simulated data. The objective of this study was twofold: first, to confirm fundamental ability of the algorithm to identify known "ground truth" parameters from a realistic but controlled dataset, and second, to quantify the estimator's robustness to sensor noise.

#### 4.1.1. Simulation Setup

A realistic flight scenario was constructed to serve as the testbed. The state trajectory (air-speed, angle of attack, etc.) was taken directly from a 200-second quasi-steady cruise segment of a real Airbus A321 flight, thereby preserving the low-excitation characteristics of the target application.

The "ground truth" aerodynamic and thrust parameters for the simulation were pre-defined, with values chosen to be representative of the A321 fleet based on the aggregated results of this study as listed in Table 4. Using this state trajectory and the ground truth parameters, a "perfect" set of noise-free forces was generated. Finally, a pseudo-QAR dataset was created by adding artificial, zero-mean Gaussian noise to all state and force signals to mimic the noise characteristics of real sensor data. The intensity of this added noise was controlled to evaluate the estimator's performance, as described in Section 4.1.3.

#### 4.1.2. Performance and Identifiability of CG-EEM

After applying the framework, the final identified parameters were used to predict the longitudinal and vertical accelerations. Figure 4 shows a comparison between these model predictions and the pseudo QAR data.

Figure 3 shows the time history of the key parameter estimates. The algorithm demonstrates excellent performance, with all parameters converging rapidly and stably from their initial 0 value towards the known ground truth values.

Table 2 provides a quantitative comparison between the final identified parameter values (averaged over the stable convergence window) and the pre-defined true values. The identified lift and thrust-related parameters are recovered with high accuracy, showing minimal bias. The drag parameters  $C_{D0}$  and  $C_{DL}$  are also identified with reasonable accuracy, though they exhibit a slightly higher bias and a significantly larger Coefficient of Variation (CV). This difference in identifiability is expected: the drag forces are much smaller than the lift forces, making their corresponding parameters inherently more sensitive to measurement noise. This result provides the quantitative justification for using a tiered CV threshold (e.g., 1% for lift parameters and 10% for drag parameters) in our convergence criteria as described in Section 3.4.

As a secondary verification, the fidelity of the final identified model was assessed by comparing its predicted accelerations against the pseudo QAR measurement data. Figure 4 shows this comparison. The model's predictions (blue line) closely track the pseudo measurements (grey line), and the residual errors shown in the bottom panels are relatively small. The higher average error in the longitudinal acceleration  $a_x$  compared to the vertical acceleration  $a_z$  is consistent with the lower signal-to-noise ratio associated with the smaller drag forces. This successful state tracking confirms that the final parameter set identified by the CG-EEM provides a high-fidelity representation of the system's dynamics.

Table 2: Verification of CG-EEM on Simulated Data

Parameter	True	Identified	Std. Dev. (in window)	CV
$C_{L0}$	0.2050	0.2016	1.83e-5	0.01%
$C_{La}$	0.0256	0.0242	0.15e-5	0.01%
$C_{LM}$	0.1570	0.1551	1.42e-5	0.01%
$C_{D0}$	0.0054	0.0063	4.23e-4	6.66%
$C_{DL}$	0.0019	0.0013	2.42e-5	3.42%
$C_{TV}$	0.0329	0.0285	2.50e-4	0.88%

#### 4.1.3. Robustness to Different Noise Level

With the model structure validated, the focus shifts to the primary objective: parameter identification. The time histories of the key aerodynamic coefficients are presented in Figure 5, demonstrating rapid and stable convergence. Table 3 lists the final parameter values, which are physically plausible and have low standard deviations within the convergence window. The combination of stable parameter convergence and accurate state tracking confirms that the framework can successfully identify the aircraft's aerodynamic characteristics from operational data.

#### 4.2. The Case for a Constant-Gain Estimator

The final framework was the result of a rigorous investigation into alternative methods and model structures. This section discusses key findings that justify our methodological choices.

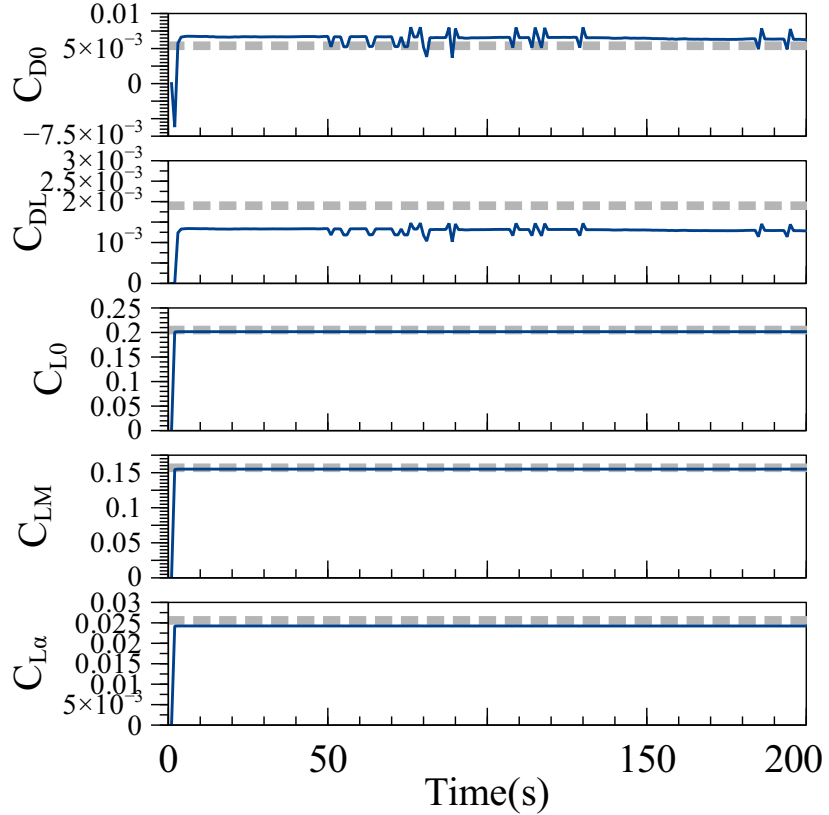


Figure 3: CG-EEM parameter convergence on simulated data. The time histories of the key aerodynamic parameter estimates (solid blue lines) are shown. The estimates demonstrate rapid and stable convergence from an initial 0 values to the known ground truth values (dashed grey lines). This verifies the fundamental integrity and accuracy of the CG-EEM algorithm.

Table 3: Final Identified Parameter Values and Standard Deviations

Parameter	Identified Value	Standard Deviation
$C_{L0}$	$2.372 \times 10^{-1}$	$8.318 \times 10^{-5}$
$C_{L\alpha}$	$2.836 \times 10^{-2}$	$6.368 \times 10^{-6}$
$C_{LM}$	$1.827 \times 10^{-1}$	$6.376 \times 10^{-5}$
$C_{D0}$	$2.803 \times 10^{-3}$	$1.299 \times 10^{-5}$
$C_{DL}$	$1.777 \times 10^{-3}$	$2.454 \times 10^{-6}$
$C_{TV}$	$2.952 \times 10^{-2}$	$1.541 \times 10^{-5}$

Note: Values are averaged over a stable convergence window (e.g., 400-500s) from the flight segment shown in Figure 5.

#### 4.2.1. Failure of Standard Recursive Least Squares

Simultaneous estimation of aircraft states and aerodynamic parameters was attempted using an Unscented Kalman Filter (UKF). However, the approach proved ineffective for the QAR data, leading to persistent parameter drift and biased state estimates, as exemplified by the longitudinal acceleration  $a_x$  error in Figure 6.

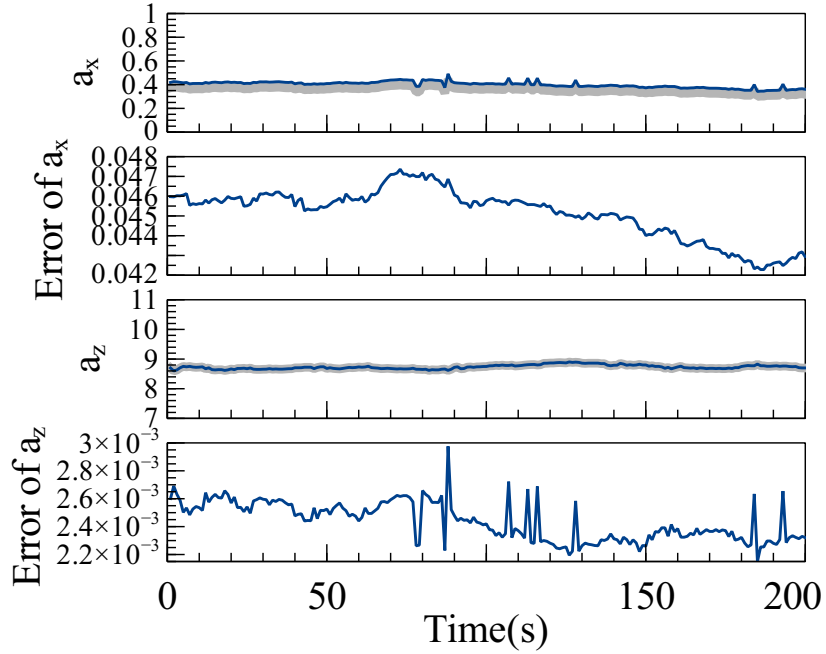


Figure 4: Fidelity of the converged model on simulated data. The top panels compare the accelerations predicted by the final identified model against the pseudo-QAR measurement data (grey). The bottom panels show the time history of the residual error. The model’s predictions closely track the noisy measurements, and the residual errors are small, confirming that the identified parameter set provides a high-fidelity representation of the system dynamics.

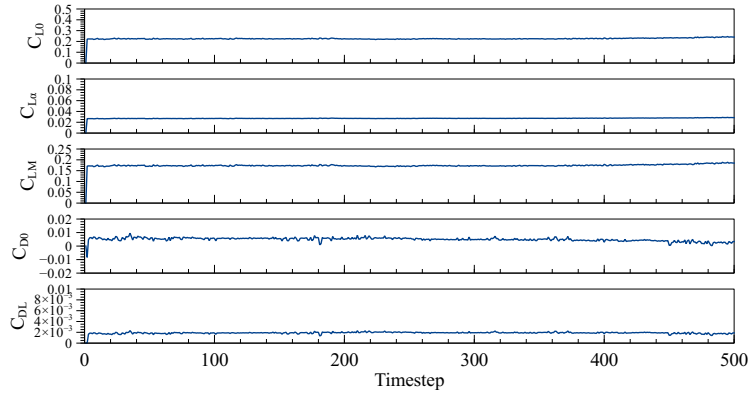


Figure 5: Time histories of key aerodynamic parameter estimates. All parameters demonstrate rapid convergence to stable and physically plausible values, confirming their identifiability.

The root of this failure was the filter’s inability to distinguish between sensor noise—particularly measurement quantization—and true model error. This was confirmed through extensive tuning of the filter’s noise covariances. Adjusting the tuning parameters created an intractable trade-off: for example, modifying the process noise for the angle of attack could reduce the  $a_x$  bias, but

only by introducing a new, unacceptable bias in the AOA estimate.

This intractable trade-off highlights the limitations of a joint estimation approach for this specific application. It motivated the decision to decouple the problem by using a dedicated parameter identification method, such as RLS, operating on a consistent set of flight data.

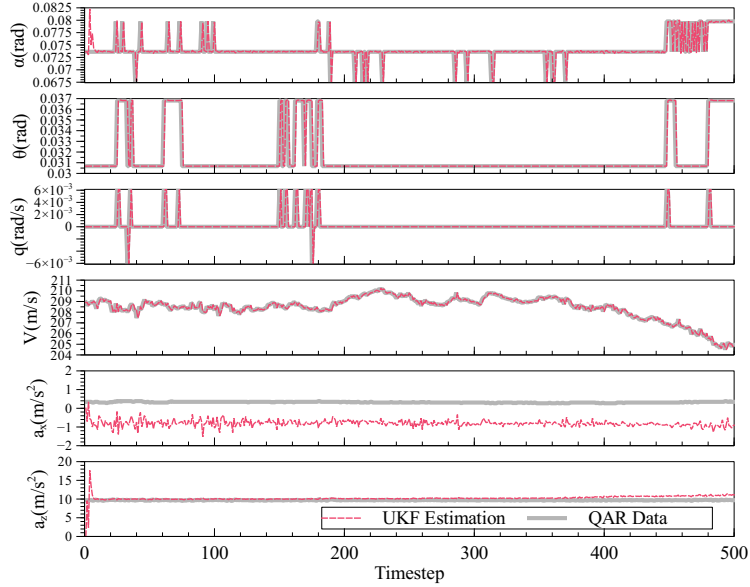


Figure 6: UKF estimation results for joint state and parameter identification. A persistent bias is evident in the longitudinal acceleration  $a_x$  estimate, a problem that could not be resolved through tuning and motivated the move to a decoupled estimation strategy.

#### 4.2.2. Necessity of the Parabolic Drag Model

To test model structure sensitivity, an alternative drag model with a linear dependency on the angle of attack ( $C_D = C_{D0} + C_{DV} \frac{V}{V_0} + C_{Da} \alpha$ ) was implemented. This model, which decouples drag from the generation of lift, proved structurally inadequate. As shown in Figure 7, the parameter estimator failed to converge, driving the drag coefficients to unstable and non-physical values.

This outcome demonstrates that the parabolic drag polar ( $C_D = C_{D0} + C_{DL} C_L^2$ ) is a critical feature of the model. Its inclusion is necessary to capture the fundamental relationship between lift and induced drag. This conclusion is well-supported by both theoretical work [16] and reference aerodynamic data for similar large commercial airliner, which show that induced drag is a dominant component of total drag [17].

#### 4.3. Application to Operational Flight Data

The robustness and consistency of the framework were validated on an extensive dataset comprising 135 flights from 33 unique Airbus A321 aircraft. The converged parameter estimates from each flight were aggregated for statistical analysis.

The statistical distributions of the key identified parameters are presented as histograms in Figure 8. The distributions for the zero-lift drag ( $C_{D0}$ ), induced drag factor ( $C_{DL}$ ), and lift curve

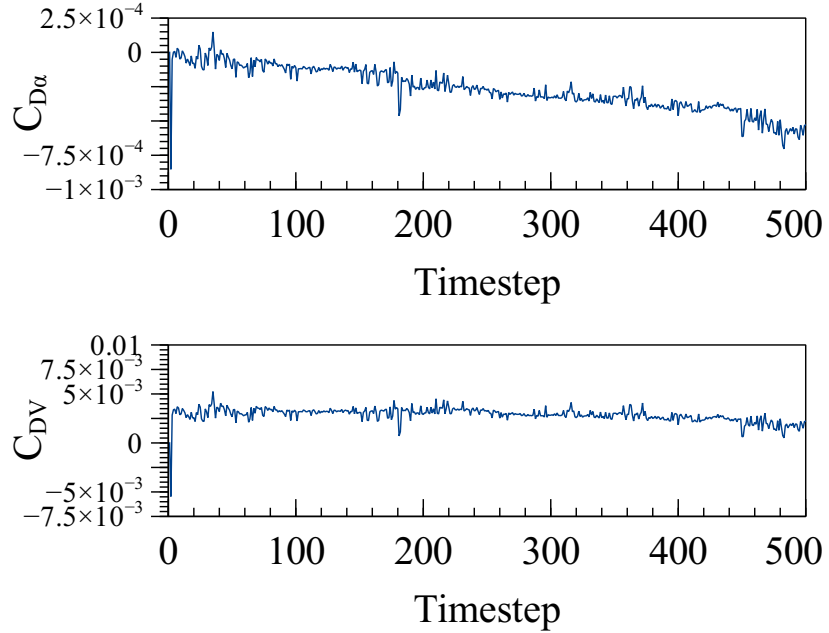


Figure 7: Parameter estimation history using the simplified linear drag model. The estimates for the drag coefficients  $C_{D\alpha}$ ,  $C_{DV}$  fail to maintain stable convergence, demonstrating the structural inadequacy of the linear model.

slope ( $C_{La}$ ) are all tightly clustered and unimodal. This demonstrates that the framework provides highly consistent results across a large and diverse set of real-world flights. A detailed statistical summary is provided in Table 4, where the mean values are shown to be physically plausible and align with expected values for this aircraft class.

Table 4: Statistical Summary of Identified Parameters for the A321 Fleet (135 flights)

Parameter	Mean	Std. Dev.	Max	Min
$C_{L0}$	0.205	0.0374	0.283	0.150
$C_{L\alpha}$	0.0256	0.0060	0.0391	0.0156
$C_{LM}$	0.157	0.0294	0.223	0.116
$C_{D0}$	0.0054	0.0076	0.0169	0.0014
$C_{DL}$	0.0019	0.0011	0.0055	0.0008
$C_{TV}$	0.0329	0.0042	0.0440	0.0251

To further assess the model’s fidelity, the correlation between the zero-lift and induced drag coefficients was examined. The scatter plot in Figure 9 shows no significant correlation between the identified values of  $C_{D0}$  and  $C_{DL}$ . This statistical independence is a critical result, as it indicates the estimator is successfully distinguishing between the two main sources of drag and not simply compensating for model errors by adjusting both parameters. This confirms the structural integrity of the underlying aerodynamic model.

This comprehensive analysis validates the framework’s potential as a reliable, low-cost tool

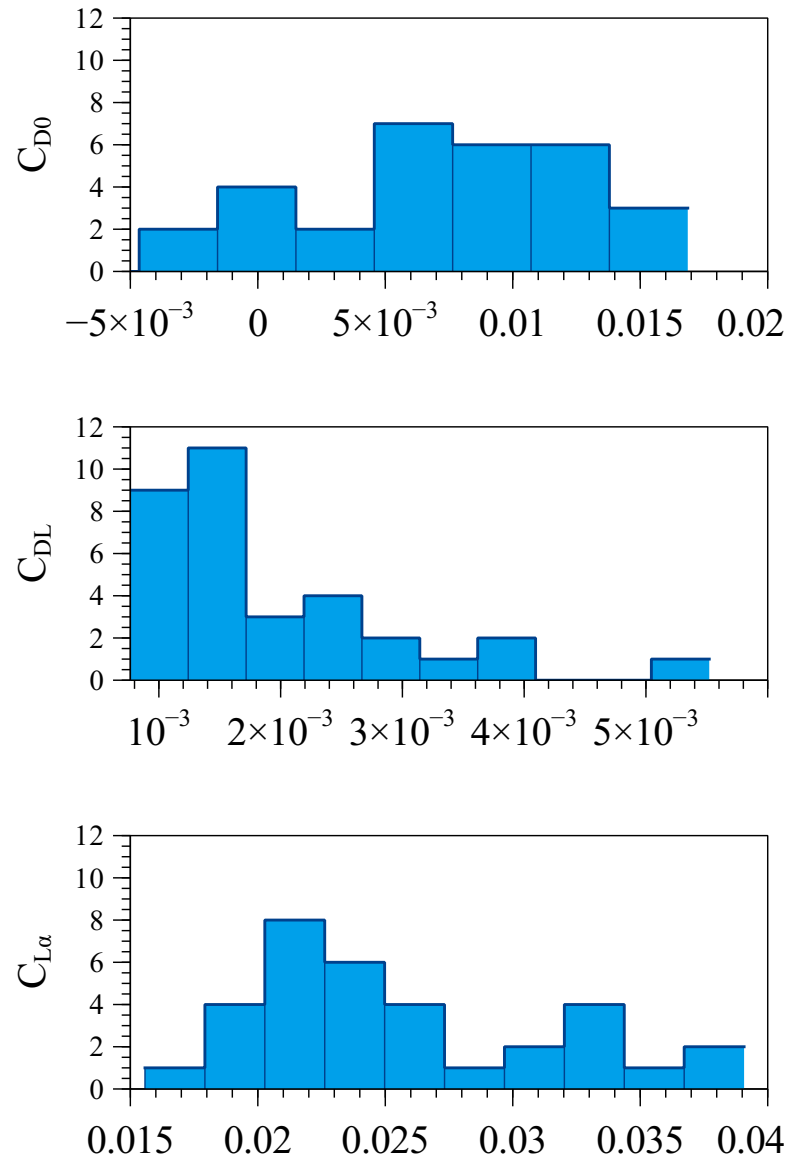


Figure 8: Statistical Distribution of Aerodynamic Parameters for the Airbus A321 Fleet (135 flights, 33 aircraft).

for monitoring fleet-wide aerodynamic performance.

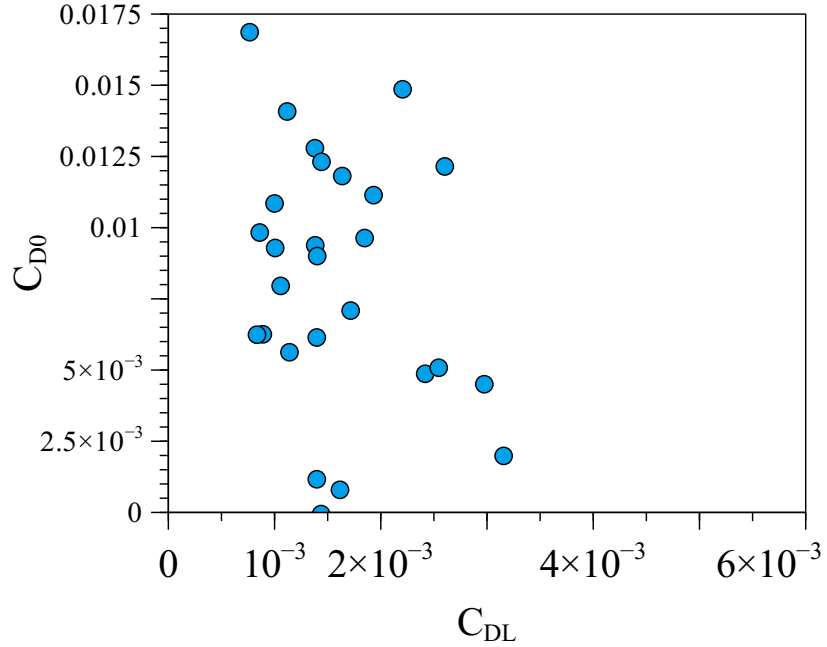


Figure 9: Correlation Analysis of Zero-Lift and Induced Drag Parameters.

#### 4.3.1. Case Study on Single Flight

#### 4.3.2. Fleet-Wide Statistical Analysis

#### 4.3.3. Framework Generality Across Multiple Aircraft Types

To validate the generality of the framework, it was applied without modification to a dataset spanning five aircraft types: the Airbus A320/A321, Boeing 737, Boeing 777, and Boeing 787. The aggregated results, shown in Table 5, confirm the robustness and physical consistency.

Table 5: Fleet-wide statistics for identified drag parameters across five aircraft types.

Aircraft Type	Flights	Mean $C_{D0}$	Std. Dev. $C_{D0}$	Mean $C_{DL}$	Std. Dev. $C_{DL}$
Airbus A320	28	0.0149	0.0032	0.0009	0.0004
Airbus A321	135	0.0054	0.0076	0.0019	0.0011
Boeing 737	10	0.0287	0.0006	0.0011	0.0001
Boeing 777	28	0.0361	0.0123	0.0026	0.0103
Boeing 787	78	0.0119	0.0017	0.0003	0.0001

As shown in Table 5, the standard deviation for the identified parameters within each fleet is small relative to the mean. This low variance demonstrates that the estimation framework is robust, providing consistent results across numerous flights of the same aircraft type.

The framework is also sensitive enough to distinguish between aircraft types based on their aerodynamic characteristics. The mean values for  $C_{D0}$  and  $C_{DL}$  are distinct for each fleet and align with physical expectations. For instance, the mean zero-lift drag ( $C_{D0}$ ) is higher for the wide-body B777 than for the narrow-body aircraft. Furthermore, the results reflect technological

differences: the composite-built, modern B787 has a significantly lower mean  $C_{D0}$  than the older B777, highlighting its superior aerodynamic efficiency. This confirms the model's ability to capture meaningful physical differences between aircraft.

## 5. Conclusions

This paper has successfully demonstrated a practical and effective framework for aerodynamic parameter estimation using readily available Quick Access Recorder (QAR) data. The methodology, centered on a Recursive Least Squares (RLS) estimator and a physically-grounded model, transforms operational data into a valuable asset for engineering analysis.

The core contribution of this work is the insight that for this specific problem, model fidelity is paramount, outweighing the benefits of advanced estimation algorithms. This was established through a series of critical findings:

1. A parabolic drag polar as equation (4), was found to be an essential model component. Its inclusion, which correctly models induced drag, was necessary for stable parameter convergence, whereas simpler linear models failed.
2. A decoupled, output-error identification approach was superior. Joint state-parameter estimation using an Unscented Kalman Filter (UKF) produced biased results, as it could not effectively disambiguate between sensor noise and model inadequacies.
3. The classical RLS estimator proved more effective than theoretically robust alternatives. Both  $H_{\infty}$  RLS and M-estimation RLS exhibited parameter drift and convergence failures, indicating that the primary challenge is not rejecting disturbances but rather fitting a well-posed model under relatively benign noise conditions.

The effectiveness and scalability of framework were validated through its application to a large, multi-fleet dataset. The analysis of 135 Airbus A321 flights produced tightly clustered, physically plausible parameter distributions, confirming the method's robustness. The framework's generality was proven by its application to four other aircraft types, where it was sensitive enough to distinguish between their unique aerodynamic characteristics—for instance, identifying the superior aerodynamic efficiency of the composite-built B787 compared to the B777.

While this framework proves highly effective for monitoring performance in cruise, its deliberate focus on longitudinal dynamics defines its current scope and presents a clear avenue for future research. Future research will focus on several key extensions to enhance the framework's capability and scope:

1. Expansion to 6-DOF: Generalizing the methodology to a full six-degree-of-freedom (6-DOF) model to identify lateral-directional coefficients and analyze more complex flight dynamics.
2. Enhanced Thrust Modeling: Replacing the current linear approximation with a high-fidelity even nonlinear thrust model that incorporates dependencies on altitude, Mach number, and engine settings (e.g., Engine Pressure Ratio).
3. Application to Other Flight Phases: Adapting the identification process to analyze data from take-off, climb, and landing, which involve significant changes in configuration and dynamics.

Ultimately, this work provides airlines with a powerful, low-cost capability for continuous fleet-wide aerodynamic health monitoring, enabling proactive maintenance, supporting fuel efficiency initiatives, and enhancing operational safety.

## Acknowledgments

This work is supported by National Key Research and Development Program of China (2023YFB4302903).

## References

- [1] N. J. Kurus and T. T. Takahashi, “Does your aircraft’s metabolism slow with time? an analysis of flight performance degradation associated with aging aircraft,” in *AIAA Scitech 2021 Forum*, p. 0460, 2021.
- [2] R. E. Maine and K. W. Iliff, “Application of parameter estimation to aircraft stability and control: The output-error approach,” tech. rep., 1986.
- [3] R. V. Jategaonkar, *Flight vehicle system identification: a time domain methodology*. American Institute of Aeronautics and Astronautics, 2006.
- [4] J. P. Slotnick, A. Khodadoust, J. Alonso, D. Darmofal, W. Gropp, E. Lurie, and D. J. Mavriplis, “Cfd vision 2030 study: a path to revolutionary computational aerosciences,” tech. rep., 2014.
- [5] Y. Tominaga, L. L. Wang, Z. J. Zhai, and T. Stathopoulos, “Accuracy of cfd simulations in urban aerodynamics and microclimate: Progress and challenges,” *Building and Environment*, vol. 243, p. 110723, 2023.
- [6] Q. Wang, R. R. Medeiros, C. E. Cesnik, K. Fidkowski, J. Brezillon, and H. M. Bleecke, “Techniques for improving neural network-based aerodynamics reduced-order models,” in *AIAA SciTech 2019 Forum*, p. 1849, 2019.
- [7] A. Mannarino and P. Mantegazza, “Nonlinear aerodynamic reduced order modeling by discrete time recurrent neural networks,” *Aerospace Science and Technology*, vol. 47, pp. 406–419, 2015.
- [8] H. Zhe, K. Yinan, Y. Weigang, and C. Gang, “Aircraft parameter estimation using a stacked long short-term memory network and levenberg-marquardt method,” *Chinese Journal of Aeronautics*, vol. 37, no. 2, pp. 123–136, 2024.
- [9] H. Geng and Y. Li, “A novel data-driven approach to parameter identification for flight simulation,” in *2023 42nd Chinese Control Conference (CCC)*, pp. 6668–6673, IEEE, 2023.
- [10] P. P. Angelov, E. A. Soares, R. Jiang, N. I. Arnold, and P. M. Atkinson, “Explainable artificial intelligence: an analytical review,” *Wiley Interdisciplinary Reviews: Data Mining and Knowledge Discovery*, vol. 11, no. 5, p. e1424, 2021.
- [11] G. Chowdhary and R. Jategaonkar, “Aerodynamic parameter estimation from flight data applying extended and unscented kalman filter,” *Aerospace science and technology*, vol. 14, no. 2, pp. 106–117, 2010.
- [12] D. Ding, K. F. He, and W. Q. Qian, “A bayesian adaptive unscented kalman filter for aircraft parameter and noise estimation,” *Journal of Sensors*, vol. 2021, no. 1, p. 9002643, 2021.

- [13] W. Qing, W. Kaiyuan, K. Yi'nan, Q. Weiqi, *et al.*, “Aerodynamic modeling and parameter estimation from qar data of an airplane approaching a high-altitude airport,” *Chinese Journal of Aeronautics*, vol. 25, no. 3, pp. 361–371, 2012.
- [14] M. R. Ananthasayanam, “Tuning of the kalman filter using constant gains,” in *Introduction and Implementations of the Kalman Filter* (F. Govaers, ed.), ch. 3, Rijeka: IntechOpen, 2018.
- [15] B. Artur, “Characteristics of the specific fuel consumption for jet engines,” tech. rep., Hamburg University of Applied Sciences, 2018.
- [16] A. M. Esteban, “A linear parameter varying model of the boeing 747-100/200 longitudinal motion,” Master’s thesis, University of Minnesota, 2001.
- [17] C. R. Hanke and D. R. Nordwall, “The simulation of a jumbo jet transport aircraft. volume 2: Modeling data,” tech. rep., NASA, 1970.